Modeling of non-isothermal CO_2 particle leaked from pressurized source: II. Behavior of single droplet

Daejun Chang*[1], Sang Heon Han[1] and Kyung-won Yang[2]

[1]*Division of Ocean Systems Engineering, Korea Advanced Institute of Science and Technology, Daejeon,Republic of Korea*
[2]*Det Norske Veritas Korea, Busan, Republic of Korea*
(Received January 9, 2012, Revised February 24, 2012, Accepted February 29, 2012)

Abstract. This study revealed the behavior of droplets formed through leak process in deep water. There was a threshold depth named the universal attraction depth (UAD). Droplets rose upward in the zone below the UAD called the rising zone, and settled down in the zone above the UAD called the settling zone. Three mass loss modes were identified and formulated: dissolution induced by mass transfer, condensation by heat transfer and phase separation by pressure decrease. The first two were active for the settling zone, and all the three were effective for the rising zone. In consequence, the life time of the droplets in the rising zone was far shorter than that of the droplets in the settling zone.

Keywords: CO_2; droplet; depletion; universal attraction depth (UAD); dissolution; condensation; isenthalpic expansion

1. Introduction

This study in a series of two papers focuses on the behavior of a droplet formed as a result of a CO_2 leak in deep water. The behavior of a bubble is addressed in Part I (Chang *et al*. 2012) where the basic principles of mass loss are elaborated, and numerical simulation is carried out for some representative cases. The readers are strongly recommended to look over the former part one since the similar principles are employed in this article.

Isothermal droplets in thermal equilibrium with the surrounding water have been studies by many research groups. In their theoretical study on the solubility of CO_2 in the ocean and its effect on CO_2 dissolution (Teng *et al*. 1996c), Teng *et al*. (1996c) estimated the shrinkage rate of CO_2 droplets, which later proved to be in a good agreement with experimental investigations. Teng and Yamasaki (2000) experimentally studied the dissolution of CO_2 drops in a high pressure counterflow water tunnel and founded out that the CO_2 drops in a moving flow dissolved much faster than the motionless drops, indicating that the mass transfer rate was enhanced due to the flow motion. Radhakrishnan *et al*. (2003) compared the theoretical and experimental dissolution rates available in literature. Kwon *et al*. (2010) theoretically calculated phase equilibrium of mixtures containing CO2 and water using nonrandom lattice fluid equation of state.

If liquid CO_2 is in contact with water at pressure greater than 44.5 bar and temperature less than

*Corresponding author, Professor, E-mail: djchang@kaist.edu

10.2°C, the hydrate form on the surface of the CO_2 droplets. A thin layer of hydrate was experimentally observed (Aya *et al*. 1992, Shindo *et al*. 1993a, Seo *et al*. 2010). Theoretical investigations were done for various cases (Shindo *et al*. 1993b, c, Teng and Kinoshita 1995, Shindo *et al*. 1996). All the studies agreed on that the formation would be completed in a few seconds with the thickness of tens of microns. Since the mutual solubility of CO_2 and water is low, the CO_2-water interface is the most probable location for hydrate formation. Moreover, the CO_2 diffusion through the solid hydrate film is too low to sustain continuous growth of the hydrate film.

In spite of the recognized existence of the hydrate, its effect on the mass transfer has been controversial. Hirai *et al*. (1996) measured the shrinkage rate of the droplets with and without the hydrate and observed that the droplets with the hydrate showed less shrinkage rate. Even under the hydrate formation conditions, a CO_2 droplet cannot be converted into a hydrate particle which just reduces the mass transfer rate (Teng *et al*. 1996b). In their experimental study, Teng and Yamasaki (2000) indicated that the hydrate did not always form on the surface of the drop in a moving flow. They observed that the hydrate seemed to develop when the CO_2 concentration the surrounded seawater was increased to a very high level.

The droplet size decreases with time since CO_2 dissolves into water. The exact dependence, however, has been an argument point. From the correlation between the Sherwood number and the Reynolds number, Hirai *et al*. (1996) deduced a non-linear correlation between the droplet size and time and provided consistent experimental observations. Other research groups, however, presented linear correlations between the droplet size and time in their theoretical (Teng *et al*. 1996a, Mori and Mochizuki 1998, Teng *et al*. 1998, Radhakrishnan *et al*. 2003) and experimental studies (Teng and Yamasaki 1998, Teng and Yamasaki 2000). An extensive review is given by Radhakrishnan *et al*. (2003).

The droplets or bubbles generated after leak process are not in thermal equilibrium with the surroundings. Since the leak process is isenthalpic, a leak in shallow water results in particles whose temperature is lower than the water by tens of degree Celsius (Chang *et al*. 2012). The heat flux into the droplets may cause mass loss from the droplet. Only few studies were available for the non-isothermal cases. Aya *et al*. (2004) performed in-situ experiment of cold CO_2 release in deep water and made very important observations. Of their four experiments, a real leak seems close to the second where an ambient liquid CO_2 was released to deep sea. The initial one mass was broken up into small droplets of a few centimeters. No theoretical study is available for non-isothermal droplets.

This study investigates the behavior of the droplet formed in deep water after leakage from a pressurized source. Following the similar principles revealed for the bubbles in the former part (Chang *et al*. 2012), the mass loss mechanism for droplets is uncovered. In spite of many in common with the bubbles, the droplets show some contrasting and different features. First of all, the evolution of a droplet is analyzed by introducing a threshold depth, called the universal attraction depth. Then, the depth is classified into the settling zone and the rising zone, followed by the modes of mass loss. Several representative cases are numerically simulated, and their results are discussed in contrast to each other.

2. Theoretical background

2.1 Evolution of droplet after leak

A leak from a high-pressure CO_2 source leads to one of various states depending on the initial state and the surrounding pressure, as described in Part I (Chang *et al*. 2012). Since enthalpy is conserved through the leak process, the state immediately after leak falls on one of the states along the constant enthalpy line in the pressure-enthalpy diagram. When the surrounding pressure is higher than the saturated liquid pressure, the leaked CO_2 is still a subcooled liquid. When the pressure is less than the saturated liquid pressure and greater than the triple-point pressure (5.18 bar), a mixture of saturated liquid and vapor is formed. The leaked CO_2 surrounded by pressure less than the triple-point pressure leads to a mixture of saturated solid and vapor. The fraction of droplets is given by the lever rule (King 1980, Chang *et al*. 2012).

$$\Gamma_{Leak,L} = \frac{h_{V,0} - h_{Source}}{h_{V,0} - h_{L,0}} = \frac{h_{V,0} - h_{Source}}{h_{LV}(P_0)} \tag{1}$$

This equation is valid under the condition that the water's hydrostatic pressure is less than the saturated liquid pressure and greater than the triple-point pressure. Depending on the leak depth the droplet immediately after leak can be lighter or heavier than the surrounding water. Fig. 1 shows the mass fraction of liquid phase and its specific gravity with depth when a leak results from a high-pressure CO_2 at 100 bar and 20°C. The mass fraction varies with the initial condition of the original CO_2 state. The specific gravity of the liquid CO_2, however, depends only on the surrounding hydrostatic pressure. That implies that there exists a critical depth below which the leak results in a liquid phase lighter than the seawater, and above which the leak forms a liquid phase heavier than the surrounding medium. The depth is a kind of attraction level to which all the droplets tend to move. For the reason, the depth is called the universal attraction depth (UAD), and the corresponding pressure and temperature of saturated CO_2 are termed the universal attraction pressure (UAP) and temperature (UAT), respectively. The exact values of the UAD, UAP, and UAT change with the density of the seawater. Considering the low compressibility of the seawater and assuming the seawater density to be equal to 1032 kg/m^3, these are estimated as follows.

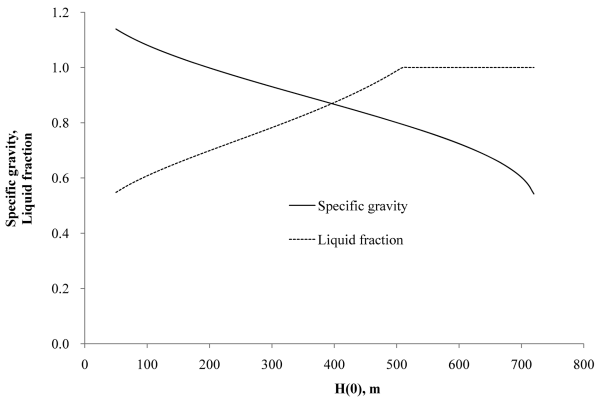

Fig. 1. Liquid fraction and specific gravity with depth after leaking from CO2 at 100 bar and 20°C

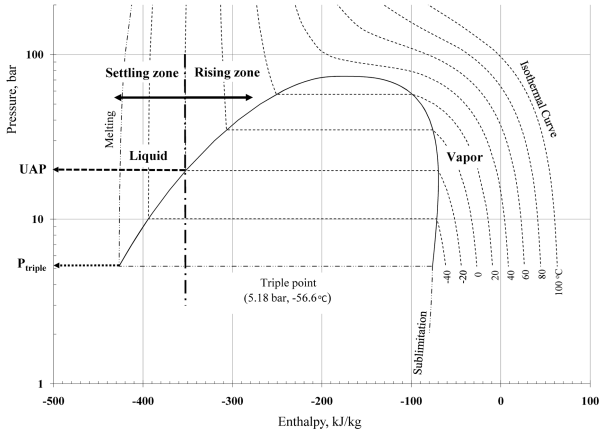

Fig. 2. Settling and rising zone divided by UAP (universal attraction pressure)

$$\text{UAD} = 198.4 \text{ m} \tag{2}$$

$$\text{UAP} = 20.9 \tag{3}$$

$$\text{UAT} = -18.1^{\circ}\text{C} \tag{4}$$

The reasoning indicates that all droplets share the common fate that they should move toward the UAD and stays there until depleted. The droplet formed above the UAD is heavier than the seawater and moves downward. To the contrary, the droplet coming into being below the UAD is lighter than the seawater and moves upward. Consequently, the zone above the UAD is the settling zone, and the zone below the UAD is the rising zone. These two zones are bounded by the UAD, equivalently UAP, as shown in Fig. 2. In consequence, the UAD is the universal destination of all the droplets.

2.2 Modes of mass loss for rising zone

The modes of mass loss for a rising droplet are similar to those for a bubble (Chang *et al*. 2012).
Mode LR.1 Dissolution induced by mass transfer
Mode LR.2 Evaporation induced by heat transfer
Mode LR.3 Phase separation induced by pressure decrease

Mode LR.1, the same as Mode V.1, is persistent for any cases since the droplet always has higher concentration than the surrounding water. Mode LR.2 is effective only if there is a temperature gradient. Note that compared with Mode V.2 heat ingress leads to a different consequence for this mode. When the droplet gains heat from the surroundings, part of it evaporates to compensate the heat gain. In most cases, the droplet is cooler than the seawater and it attracts heat from the surrounding. In unusual cases where the droplet is hotter than the sea water, it loses heat which contributes to the subcooling of the droplet. Mode LR.3 obeys the same principle that Mode V.3 does. As the rising droplet experiences pressure drop, there occurs phase separation of a vapor phase from the liquid phase. Consequently, the droplet loses the vapor part which is expected to detach from the droplet. The vapor fraction generated by Mode LR.3 is estimated by the lever rule

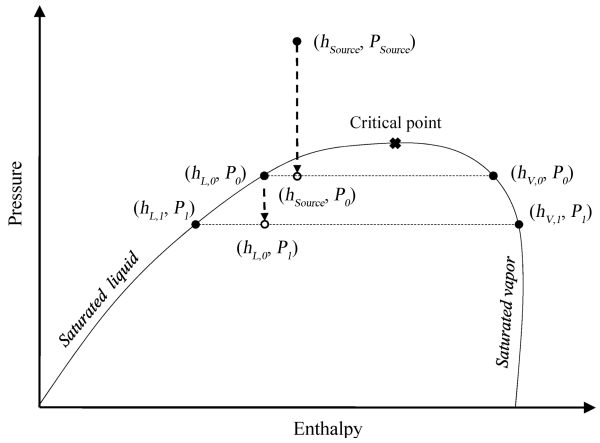

Fig. 3. New vapor-liquid equilibrium caused by change in pressure for rising zone

(King 1980, Chang *et al*. 2012). Considering Fig. 3, the vapor fraction is given by the equation.

$$\Gamma_V = \frac{h_{L,0} - h_{L,1}}{h_{V,1} - h_{L,1}} = \frac{h_{L,0} - h_{L,1}}{h_{LV}(P_1)} \tag{5}$$

In reality, the droplet movement is far slower than the phase separation, and this flashing process occurs continuously rather than the discrete way which was taken for the convenience of explanation. That is, the droplet follows the saturated liquid curve, generating the vapor.

2.3 Modes of mass loss for settling zone

In the settling zone, the droplet moves downward and experiences an increase in pressure with time. Since the pressure always increases with depth (equivalently time), the phase separation induced by pressure decrease never occurs. Consequently, only two modes are effective and are the same as Modes LR.1 and Mode LS.2.

Mode LS.1 Dissolution induced by mass transfer

Mode LS.2 Evaporation induced by heat transfer

Since the droplet in this zone is a saturated liquid, its temperature that is the saturation temperature at the leak pressure is less than the saturation temperature at the UAP. Consequently, the magnitude of heat transfer from the surrounding to the droplet, causing the droplet temperature, decreases with depth. Fig. 4 shows the effect of the two modes. Just after leak, the droplet is at Point ($h_{L,0}$, P_0). Because of the settling motion, the pressure is increased from P_0 to P_1. If there were not for Mode LS.2, the resulting state would be Point ($h_{L,0}$, P_1). The heat influx through Mode LS.2 increases the enthalpy of the droplet, leading the state to Point ($h_{L,1}$, P_1).

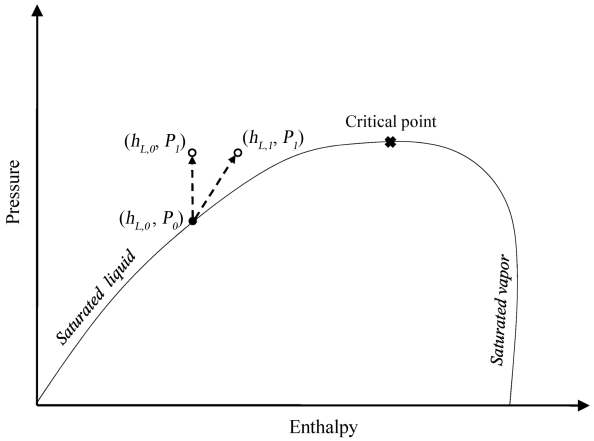

Fig. 4. New liquid state caused by change in pressure for settling zone

3. Formulation

3.1 Assumptions

In overall, the same approach as for the bubble (Chang *et al*. 2012) is taken in this study. Fig. 5 shows the definition of variables. The droplet is situated at depth H(t). Its temperature is different from that of the surrounding water, and so are the viscosity and the density. Due to the difference in density, it rises with velocity $u_L(t)$. Of course, the moving velocity is downward in the settling zone. For the rising zone, $\Delta m_{L,R,M}(t)$, $\Delta m_{L,R,T}(t)$ and $\Delta m_{L,R,P}(t)$denote the mass loss of Modes LR.1, LR.2, and LR.3, respectively. For the settling zone, $\Delta m_{LS,M}(t)$ and $\Delta m_{LS,T}(t)$ are the loss of Modes LS.1 and LS.2, respectively. Mass losses are taken positive. The following assumptions are employed on the \ basis of the reasoning mentioned previously.

A1. A droplet is formed from a liquid jet via isenthalpic expansion and initially at a saturated liquid state when the surrounding pressure is less than the saturated pressure.

A2. The droplet is placed in an infinite large quiescent flow field.

A3. The shape of the droplet is spherical for mass transfer estimation. For estimation of the

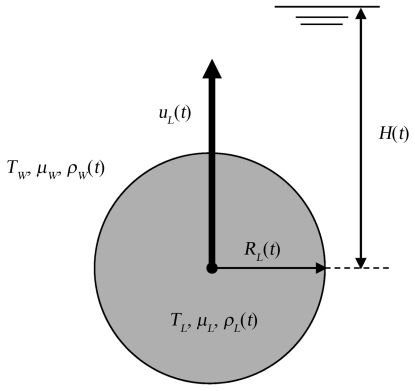

Fig. 5. Definition of state variables

terminal velocity, deformation of the droplet is considered.

A4. The droplet is free of ice or hydrate formation.

A5. The mass reduction rate due to Mode LR.1 or LS.1 is constant.

A6. For the rising zone the mass loss due to Mode LR.1 is independent of Modes LR.2 and LR.3. In an analogous way, for the settling zone the mass loss due to Mode LR.1 is independent of Modes LR.2.

A7. When the heat ingress via Mode LR.2 is greater than Mode LR.3 for the rising zone, the residual heat results in an increase in the temperature of the droplet. That is the case for the settling zone.

A8. Once the vaporized CO_2 is formed, it separates from the droplet and immediately disperses into the surrounding medium.

3.2 Mode LR.1 or LD.1 dissolution induced by mass transfer gradient

This mode is due to the difference in CO_2 concentration between the droplet and the surrounding seawater. Analogous to the bubble, the mass transfer from the droplet is modeled by the following equations.

$$J_{L^*,M}(t) = Wh_{L^*,M}(c^{\#} - c^{\infty}) \tag{6}$$

$$\Delta m_{L^*,M}(t) = A(t) J_{V,M}(t) \Delta t \tag{7}$$

$$\frac{d}{dt}(m_L) = -A(t) J_{L,M}(t) \tag{8}$$

For a spherical droplet under constant pressure circumstance, Eq. (8) reduces to the expression.

$$\frac{dR_L}{dt} = -\frac{Wh_{L^*,M}(c^{\#} - c^{\infty})}{\rho_L} \tag{9}$$

Various theoretical and experimental investigations maintained that the reduction rate is constant (Radhakrichnan *et al*. 2003), implying that the radius of the droplet linearly decreases with time.

$$R_L(t) = R_L(0) - \Phi_{L^*,M} t \tag{10}$$

Based on the experimental investigation of Teng and Yamasaki (2000) the following correlation is taken for this study.

$$\Phi_{LR,M} = \Phi_{LS,M} = (1,512 - 5.03 \cdot 10^{-3} P + 0.203 T_W - 8.90 \cdot 10^{-3} T_W^2) \cdot 10^{-6} \text{ m/s} \tag{11}$$

The dissolved mass due to the concentration gradient is given by the equation.

$$\Delta m_{L^*,M}(t) = A(t) J_{L^*,M}(t) \Delta t = A(t) \rho_L(t) \Phi_{L^*,M} \Delta t \tag{12}$$

3.3 Mode LR.2 or mode LS.2 evaporation induced by heat transfer

The significant temperature difference between the droplet and the surrounding seawater causes heat flux into the droplet.

$$J_{L^*,T}(t) = h_{L^*,T}(t)(T_W^{\infty} - T_L) \tag{13}$$

Here, L^* is either LR or LS since this mode is effective both the rising and settling zones. The evaporation mass due to the heat ingress, $\Delta m_{L^*,T}(t)$, for time interval Δt is given by dividing the heat ingress by heat of vaporization.

$$\Delta m_{L^*,T}(t) = \frac{A(t)J_{L^*,T}(t)}{h_{LV}(t)} \tag{14}$$

The same correlations as in Part I (Chang *et al*. 2012) are taken for this study.

$$Nu = 1 + (1 + Pe)^{1/3} \tag{15}$$

$$Nu = \frac{2R_V h_{V,T}}{k_W} \tag{16}$$

$$Pe = RePr \tag{17}$$

$$Pr = \frac{\mu_W C_{P,W}}{k_W} \tag{18}$$

$$Re = \frac{2R_V \rho_W u_V}{\mu_W} \tag{19}$$

3.4 Mode LR.3 phase separation induced by pressure decrease

The pressure decrease caused by a movement with velocity $u_L(t)$ for time interval Δt is given by the equation.

$$\Delta P_{L,P}(t) = g\rho_W u_L(t)\Delta t \tag{20}$$

Consider the isenthalpic transition from Point ($h_{L,n}$, P_n) by the pressure difference to Point ($h_{L,n}$, P_{n+1}) as shown in Fig. 6. As explained in Eq. (1), the mass fraction of the condensed liquid is given by the lever rule.

$$\Gamma_V(n, n+1) = \frac{h_{L,n} - h_{L,n+1}}{h_{V,n+1} - h_{L,n+1}} = \frac{h_{L,n} - h_{L,n+1}}{h_{LV}(P_{n+1})} \tag{21}$$

The evaporation mass loss due to the pressure change, $\Delta m_{L,P}(t)$, for time interval Δt is given by multiplying the droplet mass by the vapor fraction ratio.

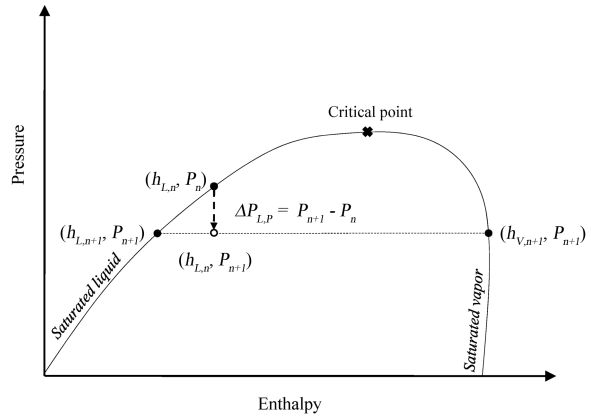

Fig. 6. Evolution of saturated state due to pressure change caused by droplet rising motion

$$\Delta m_{V,P}(t) = m_V(t)\Gamma_L(n, n+1) \tag{22}$$

The mass change due to Mode LR.3 is proportional to the volume while those due to Modes LR.1 and LR.2 increases with the surface area.

3.5 Terminal velocity

The same correlation as for the bubble (Chang *et al*. 2012) is used for the terminal velocity of a droplet.

$$u_L = \frac{\mu_W}{2\rho_W R_L} Mo^{-0.149}(J - 0.857) \tag{23}$$

$$Mo = \frac{g\mu_V^4(\rho_W - \rho_V)}{\rho_W^2 \sigma^3} \tag{24}$$

$$J = \begin{cases} 0.94\Theta^{0.757} & 2 < \Theta \le 59.3 \\ 3.42\Theta^{0.441} & \Theta > 59.3 \end{cases} \tag{25}$$

$$\Theta = \frac{4}{3} Eo\, Mo^{-0.149}\left(\frac{\mu_L}{\mu_W}\right)^{-0.14} \tag{26}$$

$$Eo = \frac{4g(\rho_W - \rho_L)R_L^2}{\sigma} \tag{27}$$

Here, Mo and Eo are the Morton number and Eötvös number, respectively. As demonstrated by Clift *et al*. (1978), the terminal velocity of tetrachloride linearly increases with the particle size for small size particles, passes through a maximum around diameter of 2 mm, and decreases to a constant velocity about 0.2 m/sec (see Fig. 7.5 of Clift *et al*. 1978). Tracking the natural CO_2

droplets (8-10 mm in diameter) by a remotely operated vehicle, Shitashima *et al*. (2008) revealed that the rising velocity was around 20-25 cm/s over a wide range of the droplet size (Fig. 6 of their study).

4. Results and discussion

4.1 Simulation cases

The same physical properties as in Part I (Chang *et al*. 2012) are taken for the seawater, as shown in Table 1. The surface tension is referred to the study by Chen *et al*. (2009), and the other physical properties are estimated from the study by Sharqawy *et al*. (2011). The leak depths taken are 50 m, 100 m, and 150 m for the settling zone, and 210 m, 250 m, 300 m, 400 m and 500 m for the rising zone. The droplet size is assumed to be 0.025 m, which is considered large enough compared with the actual observation (Aya *et al*. 2004, Shitashima *et al*. 2008). Since, the reduction rate is about $\Phi_{L^*,M} = 2.55 \cdot 10^{-6}$ at the UAP, it would take about 1000 second for the droplet to deplete with only Mode LR.1 or LS.1 effective.

4.2 Droplets in settling zone

The droplets in this zone fall down toward the UAD, as shown in Fig. 7. Once the droplets reach the UAD, they stay there to depletion. The normalized mass decreases with time, as shown in Fig. 8. All the droplets vanish around 10000 seconds, implying that only Mode LS.1 is effective with the other mode inactive. Fig. 9 shows the magnitude of Mode LS.2 normalized by Mode LS.1. Mode LS.2 is dominant in the early stage of settling and becomes insignificant after 150 seconds. This is because the temperature difference rapidly decreases with time, as shown in 10. After 150 seconds, all the droplets are in virtual thermal equilibrium with the surrounding seawater.

4.3 Droplets in rising zone

The droplets in the rising zone have shorter life time than those in the settling zone. Compare Fig. 11

Table 1 Properties of seawater

Parameter	Notation	Value		Reference
Temperature of seawater	T_W	10	^oC	
Salinity		30	g/kg	
Viscosity of seawater	μ_W	0.001382	kg/m/s	Sharqawy *et al*. 2011
Density of seawater	ρ_W	1023	kg/m^3	Sharqawy *et al*. 2011
Specific heat of seawater	$C_{P,W}$	4022	J/kg/^oC	Sharqawy *et al*. 2011
Thermal conductivity of seawater	k_W	0.587	W/m/^oC	Sharqawy *et al*. 2011
Prandtl number	Pr	9.47		Sharqawy *et al*. 2011
Surface tension	σ	0.03	N/m	Chen *et al*. 2009

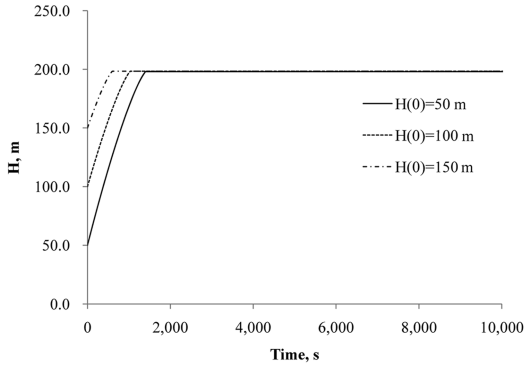

Fig. 7. Position with time in settling zone

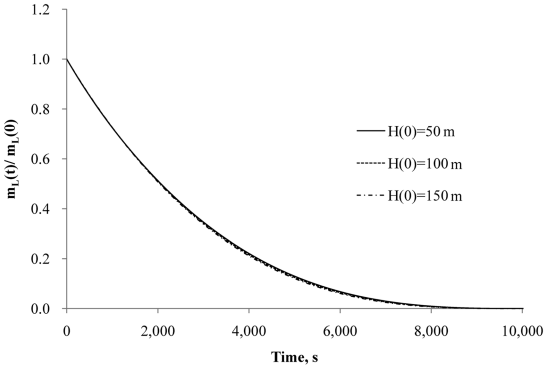

Fig. 8. Instant mass with time in settling zone

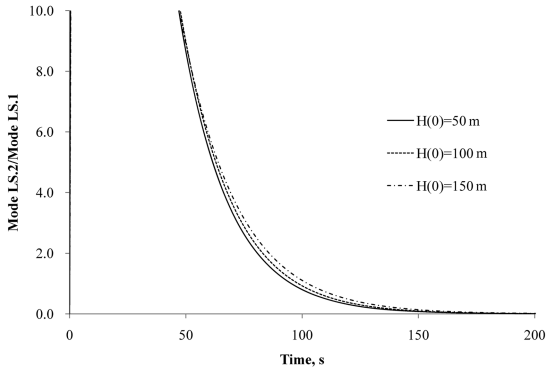

Fig. 9. Ratio of Mode LS.2 to Mode LS.1 with time in settling zone

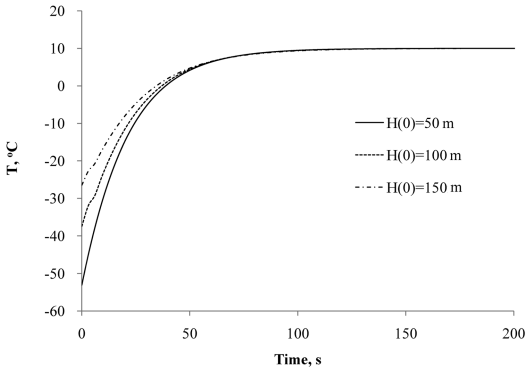

Fig. 10. Temperature with time in settling zone

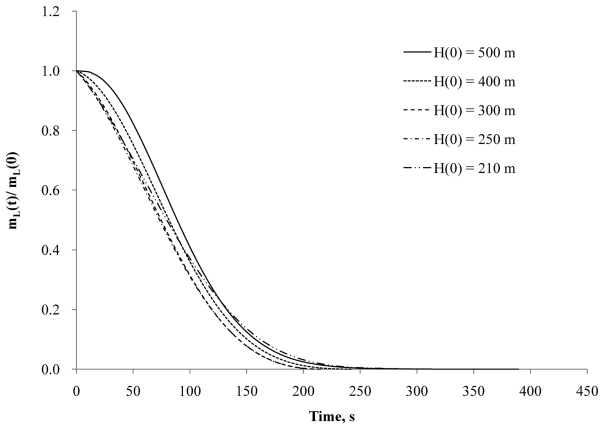

Fig. 11. Instant mass with time in rising zone

with Fig. 8. The life time of the former is about 200 seconds while that of the latter is about 800 seconds. This is because all the modes of mass loss are working, as described below. The droplets in this zone are subject to the three modes of mass loss. As they rise, the droplets follow the saturated temperature to the surrounding pressure, as shown in Fig. 12. The droplet with H(0) = 500 m is

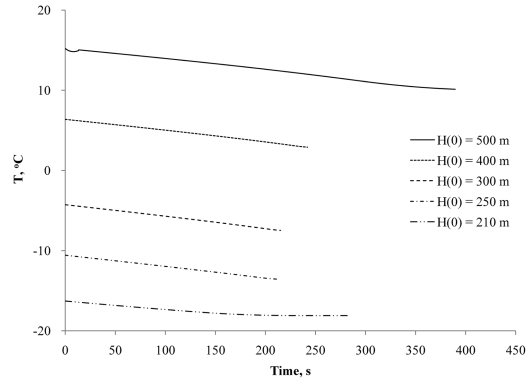

Fig. 12. Temperature with time in rising zone

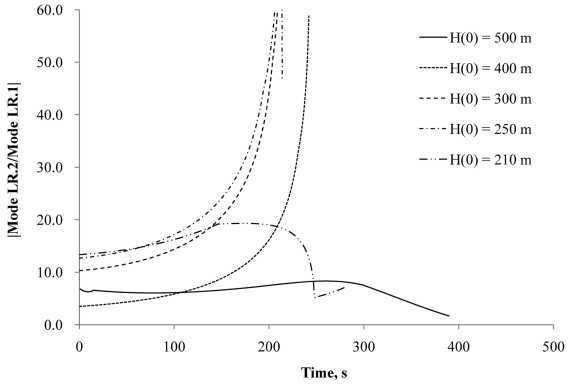

Fig. 13. Ratio of Mode LR.2 to Mode LR.1 with time in rising zone

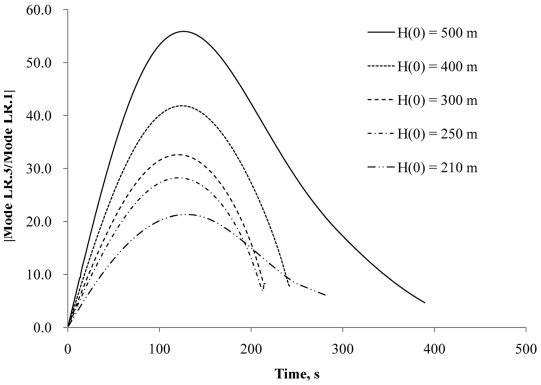

Fig. 14. Ratio of Mode LR.2 to Mode LR.1 with time in rising zone

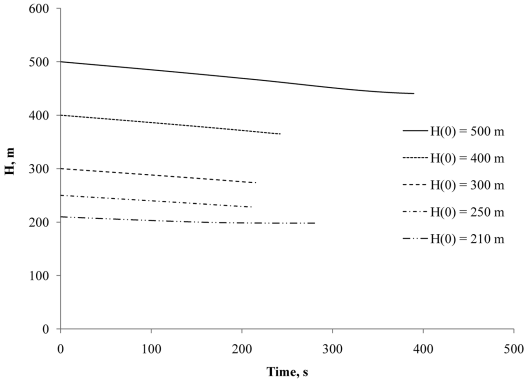

Fig. 15 Position with time in rising zone

hotter than the water. During the early short period, condensation via Mode LR.2 ($\Delta m_{LR,T}(t) < 0$) is larger than the vapor generation via Mode LR.3, and the droplet releases an amount of heat causing subcooling below the saturated temperature. The small dent on the curve is formed for the reason. Mode LR.3, however, soon overcomes Mode LR.2, and the droplet follows the saturated temperature curve. For the other H(0)'s, the droplets is cooler than the water, and even Mode LR.2 contributes to the mass loss together with Mode LR. 3. Figs. 13 and 14 show the magnitude of Modes LR.2 and LR.3 normalized by Mode LR.1. Over the life time, the two modes are much more influential than Mode LR.1. Mode LR.2 is active even in the later stage. This is because the temperature difference is still significant until the droplets vanish. Fig. 15 shows the depth of the droplets in the rising zone. All the droplets are moving upward to the UAD. All droplets disappear before touching the UAD except for the droplet with H(0) = 210 m which stays at the UAD until depleted.

5. Conclusions

Analogous to the analysis of bubbles, the three modes of mass loss from non-isothermal droplets

were identified. Dissolution was induced by mass transfer while evaporation and phase separation were caused by heat transfer and pressure decrease, respectively. The pressure-enthalpy diagram was employed to interpret the last mode. Due to the isenthalpic expansion from the high-pressure source and the varied specific gravity, the universal attraction depth (UAD) about 200 m was identified, and the two zones were defined: the settling zone above the UAD and the rising zone below the UAD. In consequence, all the droplets tend to move toward the UAD once they are formed. The activity of the three modes is not uniform in the two zones. The dissolution and evaporation modes were active for the settling zone, and all the three were effective for the rising zone. In consequence, the life time of the droplets in the rising zone was far shorter than that of the droplets in the settling zone.

Much research effort will be requested to reveal more accurate anticipation of CO_2 leak in deep water. Many aspects are still unclear: existence of the hydrate layer, the ice formation, the particle size distribution just after the leak, etc. The most challenging issue is the behavior of the aggregate of the droplets and bubbles. As they rise and falls in group, they will interact with each other changing themselves and their environment, to name a few, their shape, the flow field around them, the CO_2 concentration in the water, and the temperature of the seawater. All these aspects should be addressed to quantify the risk to safety and environment and to come up with appropriate safety measures.

Acknowledgements

This research was supported by a grant from the LNG Plant R&D Center funded by the Ministry of Land, Transportation and Maritime Affairs (MLTM) of the Korean government.

References

Aya, I., Yamane, K. and Yamada, N. (1992), "Simulation experiment of CO2 storage in the basin of deep ocean", *Energ. Convers. Manage*., **36**(6-9), 485-488.

Aya, I., Kojima, R., Yamane, K., Shiozaki, K., Brewer, P.G. and Peltzer, E.T. (2004), "In situ experiments of cold CO_2 release in mid-depth", *Energy*, **29**(9-10), 1499-1509.

Chang, D., Han, S.H. and Yang, K. (2012), "Modeling of non-isothermal CO2 particle leaked from pressurized source: I. Behavior of single bubble", *Ocean Syst. Eng*. (submitted).

Chen, B., Nishio, M., Song, Y. and Akai, M. (2009), "The fate of CO2 bubble leaked from seabed", *Energ.,Procedia*, **1**(1), 4969-4976.

Clift, R., Grace, J.R. and Weber, M.E. (1978), *Bubbles, drops, and particles*, Dover Publication Inc., New York.

Hirai, S., Okazaki, K., Araki, N., Yazawa, H., Ito, H. and Hijikata, K. (1996), "Transport phenomena of liquid CO2 in pressurized water flow with clathrate-hydrate at the interface", *Energ. Convers. Manage*., **37**(6-8),1073-1078.

King, C.J. (1980), *Separation Processes*, 2nd Ed., McGraw-Hill book company, New York.

Kwon, C.H., Lee, C. and Kang, J.W. (2010), "Calculation of phase equilibrium for water+carbon dioxide system using nonrandom lattice fluid equation of state", *J. Chem. Eng. Korea*, **27**(1), 278-283.

Mori, Y.H. and Mochizuki, T. (1998), "Dissolution of liquid CO2 into water at high pressures: a search for the mechanism of dissolution being retarded through hydrate-film formation", *Energ. Convers. Manage*., **39**(7), 567-578.

Radhakrishnan, R., Demurov, A., Herzog, H. and Trout, B.L. (2003), "A consistent and verifiable macroscopic model for the dissolution of liquid CO2 in water under hydrate forming conditions", *Energ. Convers.*

Manage., **44**(5), 771-780.
Sharqawy, M.H., Lienhard J.H. and Zubari, S.M. (2011), "On exergy calculations of seawater with applications in desalination system", *Int. J. Therm. Sci*., **50**(2), 187-196.
Shindo, Y., Fujioka, Y., Yanagisawa, Y., Hakuta, T. and Komiyama, H. (1993a), "Formation and stability of CO_2 hydrate", *Proceedings of the 2nd International Workshop between CO2 and Ocean*, Japan, April.
Shindo, Y., Lund, P.C., Fujioka, Y. and Komiyama, H. (1993b), "Kinetics and mechanism of the formation of CO_2 hydrate", *Int. J. Chem. Kinetics*, **25**, 777-782.
Shindo, Y., Lund, P.C., Fujioka, Y. and Komiyama, H. (1993c), "Kinetics of formation of CO2 hydrate", *Energ. Convers. Manage*., **34**(9-11), 1073-1079.
Shindo, Y., Sakaki, K., Fusioka, Y. and Komiyama, H. (1996), "Kinetics of the formation of CO2 hydrate on the surface of liquid CO2 bubble in water", *Energ. Convers. Manage*., **37**(4), 485-489.
Shitashima, K., Maeda, Y., Koike, Y. and Ohsumi, T. (2008), "Natural analogue of the rise and dissolution of liquid CO2 in the ocean", *Int. J. Greenh. Gas Con*., **2**(1), 95-104.
Seo, M.D., Seo, S.H., Kang, J.W. and Lee, C.S. (2010), "Interfacial equilibrium and mass transfer from liquid CO2 disks through hydrate films", *Energ. Convers. Manage*., **51**(4), 710-713.
Teng, H., and Kinoshita, M. (1995), "Hydrate formation on the surface of a CO2 bubble in high-pressure, lowtemperature water", *Chem. Eng. Sci*., **50**(4), 559-564.
Teng, H., Yamasaki, A. and Shindo, Y. (1996a), " Stability of the hydrate layer formed on the surface of a CO2 bubble in high-pressure, low-temperature water", *Chem. Eng. Sci*., **51**(22), 4979-4986.
Teng, H., Masutani, S.M., Kinoshita, C.M. and Nihous, G.C. (1996b) "Solubility of CO2 in the ocean and its effect on CO2 dissolution", *Energ. Convers. Manage*., 37(6-8), 1029-1038.
Teng, H., Yamasaki, A. and Shindo, Y. (1996c), "The fate of liquid CO2 disposed of in the ocean", *Energy*, **21**(9), 765-774.
Teng, H. and Yamasaki, A. (1998), "Mass transfer of CO2 through liquid CO2-water interface", Int. *J. HeatMass. Tran*., **41**(24), 4315-4325.
Teng, H. and Yamasaki, A. (2000), "Dissolution of buoyant CO2 drops in a counterflow water tunnel simulating the deep ocean waters", *Energ. Convers. Manage*., **41**(9), 929-937.

Nomenclature

Alphabets	
A	Surface area of the droplet, m^2
B	Reduction rate of the droplet radius, m/s
C	Heat capacity, $J(/(\mathrm{kg}\cdot{}^{\circ}\mathrm{C})$
$c^{\#}$	CO_2 concentration on the interface between the bubble and the water, mol/m^3
c^{∞}	CO_2 concentration in the far field, mol/m^3
u_V	Terminal velocity of a CO_2 droplet, m/s
H	Depth, m
$h_{L,M}$	Mass transfer coefficient, m/s
$h_{L,i}$	Enthalpy of liquid phase at state i, J/kg
h_{Source}	Enthalpy of high-pressure source, J/kg
$h_{V,i}$	Enthalpy of liquid phase at state i, J/kg
$h_{LV}(\mathrm{P}_i)$	Heat of vaporization at pressure , Pi J/kg
g	Gravitational acceleration, m/s^2
$J_{V,M}$	Mass flux, $kg/(m^2\cdot s)$
$J_{V,T}$	Heat flux, $J/(m^2\cdot s)$
k	Thermal conductivity, $J/(m\cdot s)$
m	Mass, kgs

$\Delta m_{V,M}$	Mass loss through Mode V.1 Dissolution induced by mass transfer, kg
$\Delta m_{V,T}$	Mass loss through Mode V.2 Condensation induced by heat transfer, kg
$\Delta m_{V,P}$	Mass loss through Mode V.3 Phase separation induced by pressure decrease, kg
P	Pressure, N/m^2
R	Radius of the droplet, m
S	State
T	Temperature, ^oC
W	Molecular weight of CO_2, kg/mol

Greeks

$\Gamma_{Lesk,L}$	Liquid mass fraction just after leak
$\Gamma_{L(i,j)}$	Liquid mass fraction over transition from State i to State j
ρ	Density, kg/m^3
σ	Surface tension, N/m

Subscripts

V	CO_2 vapor phase
W	Water phase